ResearchGate

See discussions, stats, and author profiles for this publication at: https://www.researchgate.net/publication/230776594

Decrystallization of Oligosaccharides from the Cellulose Iβ Surface with Molecular Simulation

ARTICLE *in* JOURNAL OF PHYSICAL CHEMISTRY LETTERS · JULY 2011

Impact Factor: 7.46 · DOI: 10.1021/jz2005122

CITATIONS
32

READS
67

4 AUTHORS, INCLUDING:

Christina M. Payne
University of Kentucky
38 PUBLICATIONS **412** CITATIONS
SEE PROFILE

Michael F Crowley
National Renewable Energy Laboratory
118 PUBLICATIONS **2,131** CITATIONS
SEE PROFILE

Gregg T. Beckham
National Renewable Energy Laboratory
93 PUBLICATIONS **2,187** CITATIONS
SEE PROFILE

Available from: Gregg T. Beckham
Retrieved on: 26 January 2016

THE JOURNAL OF PHYSICAL CHEMISTRY Letters

LETTER

pubs.acs.org/JPCL

Decrystallization of Oligosaccharides from the Cellulose Iβ Surface with Molecular Simulation

Christina M. Payne,*[,§] Michael E. Himmel,[§] Michael F. Crowley,[§] and Gregg T. Beckham*[,†,‡]

[§]Biosciences Center and [†]National Bioenergy Center, National Renewable Energy Laboratory, Golden, Colorado 80401, United States

[‡]Department of Chemical Engineering, Colorado School of Mines, Golden, Colorado 80401, United States

Supporting Information

ABSTRACT: Bundles of cellulose polymers in plant cell walls exhibit a robust network of hydrogen bonds and hydrophobic interactions that must be overcome to decrystallize and hydrolyze the individual polymers to sugars. To investigate the molecular interactions that impart recalcitrance and insolubility to cellulose, we use simulation to determine the decrystallization work, a fundamental, yet experimentally inaccessible measurement, of cello-oligomers from the middle and edge of the hydrophobic face of cellulose Iβ. We demonstrate that cellobiose and cellotetraose decrystallization work does not depend on the position of the oligomer on the crystal surface but that larger oligomers are more difficult to decrystallize depending on the number of intralayer neighbors due to a larger number of stabilizing intralayer hydrogen bonds. The presented results are relevant to mesoscale, morphology-based models of cellulose deconstruction, understanding the molecular details of cellulose decrystallization and insolubility, and quantifying the oligomer length scale upon which short cellulose chains become inhibitory to enzymatic deconstruction of cellulose.

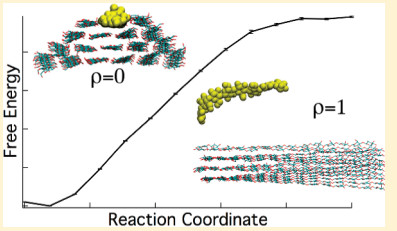

SECTION: Biophysical Chemistry

Cellulose is the most abundant biological material on Earth and is the linear polymer of β1,4-D-glucose.[1] Cellulose comprises the primary structural component of plant cell walls, giving rise to its vast abundance. The chemical and physical properties of cellulose, in combination with other cell wall polymers, provide plants with a highly evolved structural defense against attack from foreign organisms on its structural sugars, which is typically termed recalcitrance.[2] These exceptional mechanical and structural properties are derived from a molecular-level network of hydrogen bonds and hydrophobic interactions present in crystalline cellulose,[3,4] making deconstruction of the polymer difficult.[5]

An open question, key to understanding cellulose, relates to the molecular reasons for cellulose recalcitrance and, generally, its insolubility as a function of oligomer length. Addressing this question requires examination of many potential factors, including entropic contributions that arise from interactions between cello-oligomers and solution and both hydrogen bonding and hydrophobic interactions in the crystal, which depend strongly on the cellulose polymorph. Multiple simulation studies have examined the molecular basis for cellulose recalcitrance.[6−19] Bergenstråhle et al. examined the contributions from hydrogen bonding and hydrophobic stacking on cellulose insolubility with small oligomers and found that both contributions favor the crystalline state.[7] In a separate study, Bergenstråhle et al. investigated the desorption of cellulose oligomers from the surface of cellulose Iβ using nonequilibrium molecular dynamics (MD), which provided insight into the interfacial desorption energy of cellulose from the hydrophilic face of cellulose Iβ.[6] Recently, we examined the decrystallization free energy of covalently attached cellulose chains from surfaces and calculated the intrinsic stability of cellulose on a monomer (cellobiose) basis as a function of polymorph and location of surface chains.[5]

Related to understanding cellulose structure and deconstruction, many groups have recently developed mesoscale, morphology-based models of cellulose deconstruction by enzymes in an effort to improve the efficiency of industrial processes to utilize cellulose as a renewable feedstock.[20−25] Developing accurate morphology-based models describing cellulose deconstruction requires quantitative knowledge of oligomer binding and reannealing to cellulose crystals as a function of morphology, which is difficult to measure experimentally. To that end, we use molecular simulations to calculate the work required to decrystallize short oligomers of cellulose from the surface of a cellulose Iβ microfibril as a function of chain location on the surface. In calculating the intrinsic work required to separate the molecule completely from the crystal, we aim to understand the factors contributing to solubility of cello-oligomers as a function of both length and position within a cellulose crystal. This information will help address the issue of cellulase inhibition by rebinding of oligomers to the crystal structure, which is relevant to building realistic morphology-based models of enzymatic cellulose deconstruction. Finally, we can extrapolate from our results what

Received: April 14, 2011
Accepted: June 2, 2011
Published: June 08, 2011

ACS Publications © 2011 American Chemical Society

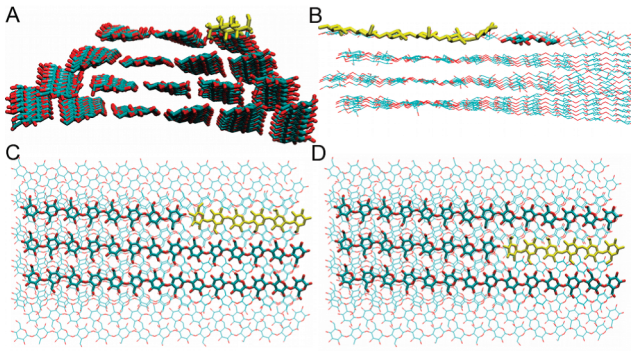

Figure 1. Definition of oligomer positions on the cellulose Iβ surface. The oligomer of interest (cellohexaose in this case) is shown in yellow. (A) Cello-oligomer in the edge conformation, end view (c-axis) (B) Cello-oligomer edge conformation, side view (a-axis). (C) Cello-oligomer in the edge conformation, top view (b-axis). (D) Cello-oligomer in the middle conformation, top view (b-axis).

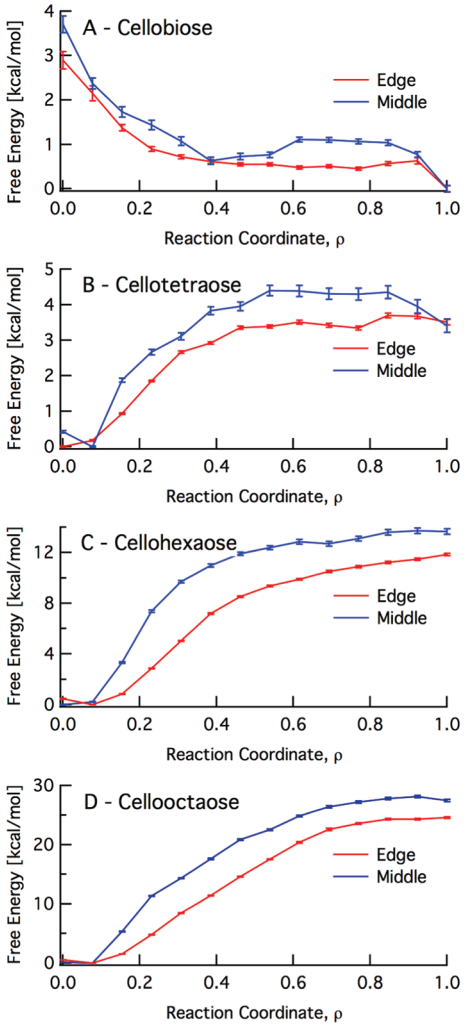

Figure 2. Potential of mean force curves for decrystallization simulations. Free energy as a function of ρ for (A) cellobiose, (B) cellotetraose, (C) cellohexaose, and (D) cellooctaose.

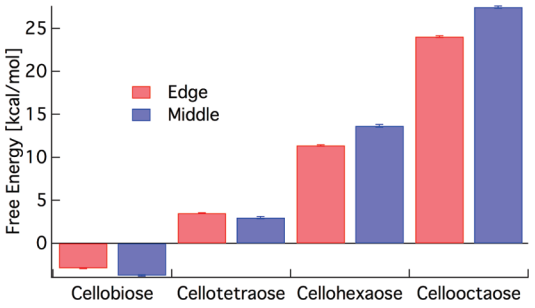

Figure 3. Free energy of decrystallization as a function of oligomer length for edge and middle position chains.

the surface of a cellulose Iβ microfibril might resemble following endoglucanase action.

We examined eight separate oligomer decrystallization scenarios, including edge and middle chains for cellobiose, cellotetraose, cellohexaose, and cellooctaose, as illustrated in Figure 1. Each of these hydrolyzed oligomers was decrystallized from the cellulose Iβ crystal from a reaction coordinate of $\rho = 0$ to 1, as defined in the Computational Methods section. Once the oligomer reaches $\rho = 1$, it has complete conformational freedom in solution. A movie of a selected trajectory illustrating decrystallization is provided in the Supporting Information.

The decrystallization free energy as a function of the reaction coordinate is given in Figure 2 for all eight scenarios. In Figure 2, there is an inflection at low values of ρ caused by the observed dislodging and annealing of the adjacent chains.[5] This phenomenon was further verified through the root-mean-square fluctuation (RMSF) calculations performed on the chains adjacent to the decrystallized oligomer, as described below. The profiles for the insoluble oligomers — cellotetraose, cellohexaose, and cellooctaose — are qualitatively similar, as expected. For cellobiose, both the middle and edge potential of mean force (PMF) profiles demonstrate that work is required to maintain native contacts in the crystal. We note that the path taken (i.e., the shape of the PMF) is not the feature of interest. Rather, we are interested primarily in the initial and final states as a measure of decrystallization work.

Figure 2 shows the work required to fully decrystallize the oligomers. Figure 3 summarizes the free energy on a length and position basis. Error bars are the standard error of the mean. The difference in free energy based on the position in the crystal (edge versus middle) is −0.8, −0.5, 2.3, and 3.3 kcal/mol in increasing order of length. From Figure 2, the shorter oligomers, cellobiose and cellotetraose, exhibit surprisingly little difference in free energy based on position. As chain length increases, the middle chain becomes increasingly difficult to remove from the cellulose crystal with respect to the edge. Generally, the results in Figures 2 and 3 overall demonstrate that interlayer interactions are a primary contribution to the decrystallization work.

However, additional contributions are evident for the larger oligomers, cellohexaose and cellooctaose. To determine the reasons for the observed free-energy differences in the longer oligomers, we examined multiple system properties. First, we calculated the RMSF of the chains adjacent to the decrystallized oligomer when all native contacts were broken to determine if the observed differences in Figure 3 arise from entropic contributions. The individual RMSF plots for each of the trajectories are shown in Figures S2 and S3 (Supporting Information). Little

dx.doi.org/10.1021/jz2005122 |J. Phys. Chem. Lett. 2011, 2, 1546–1550

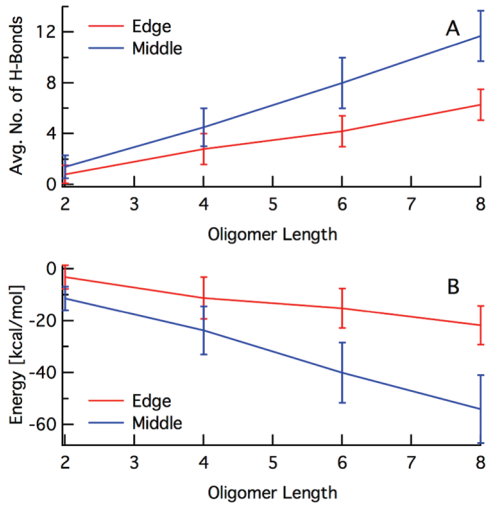

Figure 4. (A) Average number of intralayer hydrogen bonds as a function of oligomer length and position in the reactant state. (B) Intralayer oligomer interaction energy as a function of length and position in the reactant state.

difference is observed between the edge and middle chains for a given oligomer length.

We also evaluated hydrogen bond behavior for the reactant state in each scenario to determine if the occupancy of intermolecular hydrogen bonds gives rise to the trends in Figure 3. This analysis included hydrogen bonds within the given chain of interest (self), within the same layer and neighboring the chain of interest (intralayer), and between layers neighboring the chain of interest (interlayer), the lattermost of which includes both conventional O−H−O and recently described "alternative" C−H−O hydrogen bonds.[10] Conventional hydrogen bond cutoffs were defined as within 3.4 Å of the donor and acceptor and 60° from linear. Figure 4a shows the average number of intralayer hydrogen bonds to the crystal for each of the reactant state oligomers. Error bars represent one standard deviation. Plots of the self and interlayer hydrogen bonds are shown in Figure S4 (Supporting Information). For cellobiose and cellotetraose, the average number of intralayer hydrogen bonds for the edge and middle chains is within 1 standard deviation. Cellohexaose and cellooctaose display greater extents of intralayer hydrogen bonding when they are in the middle position. We find that interlayer hydrogen bonding to the chain of interest varies little as a function of position and chain length, and not surprisingly, the self-hydrogen bonding increases linearly with chain length and is not an apparent function of position.

To further investigate the trend of positional dependence for cellobiose and cellotetraose, we calculated the intralayer interaction energies of the chain of interest with its neighboring glucose units. The results of this analysis are shown in Figure 4b. Again, we find that the intralayer interaction energies for the chains of interest in the reactant state show that the edge and middle cellobiose and cellotetraose have similar energetic barriers to decrystallization. Plots of the interaction energies, separated into van der Waals and electrostatics, are shown in Figure S5 (Supporting Information).

The primary aim of this study is to provide a molecular understanding of cellulose insolubility and recalcitrance and, more specifically, insight into the thermodynamics of cellulose oligomers interacting with cellulose crystals. Experimental solubility measurements have been conducted for short oligomers of cellulose in water, which typically show that solubility decreases rapidly for cellodextrins larger than cellotriose.[26,27] However, thermodynamic measurements of cellulose oligomer binding and reannealing to cellulose crystals have not been reported to our knowledge, though this quantity is of fundamental importance for enzymatic deconstruction of plant cell walls. Isothermal titration calorimetry or similar thermodynamic measurements would quantify the binding affinity of cellulose oligomers (or oligomers of hemicellulose sugars) to cellulose crystals as an ensemble measurement. These types of measurements could aid explanations of reduced conversion efficiencies at high solids loadings where the presence of cellulose and hemicellulose oligomers is likely significant.[41,42] From our study, the simulation results suggest that cellobiose is readily removed from the crystal surface to bulk solution regardless of position on the cellulose microfibril. Interestingly, though a significant contribution to decrystallization work is from hydrophobic interlayer stacking,[5,7] our results also show that intralayer hydrogen bonding is a significant contributor to increased free energy of decrystallization for larger oligomers, which has implications in the molecular origins of biomass recalcitrance and cellulase inhibition by annealing of oligomers to the surface of cellulose. Also of interest, while this study focuses on the decrystallization of origin chains as opposed to the layer chains constructing cellulose Iα, we note that because interlayer hydrogen bonding plays a small role in differentiating the free energy of decrystallization, the results found here for cellulose Iβ are likely relevant to the cellulose Iα construct.

From a computational standpoint, calculations of the decrystallization free energy for cello-oligomers to date have used more restrictive reaction coordinates to characterize solubility in terms of hydrogen bonding and hydrophobic stacking interactions for efficient convergence. The choice of fraction of native contacts as a reaction coordinate requires significantly longer simulations, but it allows for complete conformational flexibility of the oligomer as it proceeds along the decrystallization trajectory. Such an approach also includes the entropic effects inherent in the decrystallized end state that are restricted by the typical distance constraint coordinates.

The difference in free energies of decrystallization calculated here and previously[5] is equivalent to the contributions from the hydrolysis of the glycosidic linkage and the entropic effects of the oligomer free in solution. Previously, we evaluated the decrystallization free energy for a nonhydrolyzed cellodecaose from cellulose Iβ being decrystallized from the middle and edge positions, as we have described here. For comparison, the PMF calculated by Beckham et al. can be divided into cellobiose units for translation into cellobiose, cellotetraose, and so forth. In so doing, we generally find the nonhydrolyzed free energy to be greater than the hydrolyzed free energy by ∼2−9 kcal/mol for a given length chain, indicating that contributions from the glycosidic linkage, constant for each case, and reduced translational, rotational, and configurational entropy of the decrystallized chain in solution are significant. Our previous study also found the nonhydrolyzed cellobiose and cellotetraose free energy of decrystallization to be virtually the same for edge and middle chains. We observe the same trend here, shown in Figure 2, further bolstering the conclusion that crystalline position for small oligomers is relatively insignificant as a barrier to decrystallization.

Related to the enzymatic deconstruction of biomass, we can extrapolate what these results might mean for the cellulose Iβ microfibril surface following endoglucanase treatments. Given

that most endoglucanases exhibit clefts for catalytic sites, as opposed to tunnels in exoglucanases, endoglucanases likely exhibit lower ligand binding free energies.[28,29] Because of the lower ligand binding free energy, we hypothesize that when endoglucanases bind to the microfibril surface, it is more likely to occur at an edge[5] or, from the current study, at an end containing mostly small oligomers. Because only the smaller oligomers are readily soluble in water, the longer oligomers remaining in the crystal would require processive enzymatic action to remove the polymer chain from the surface. Detailed models of nonprocessive enzymatic action have yet to be developed; however, the results presented here, combined with absolute binding free-energy calculations of cellulose oligomers to endoglucanase clefts, are key studies needed to improve our understanding of enzymatic biomass deconstruction with the aim of designing more efficient biofuels processes.

In summary, we have conducted free energy simulations to calculate the work required to decrystallize cello-oligomers of varying lengths and position on a cellulose Iβ crystal. Our results demonstrate that while hydrophobic stacking interactions contribute greatly to the free energy of decrystallization, larger oligomer chains with more intralayer contacts are more difficult to decrystallize. Cellobiose and cellotetraose, however, require similar amounts of work to decrystallize the oligomer as a result of similar intralayer hydrogen bonding patterns, regardless of surface location. The results also suggest oligomer solubility below cellotetraose due to the work requirement, which is in agreement with experiment. Results from this study are crucial for continued development of mesoscale, morphology-based kinetic models of lignocellulosic biomass deconstruction, leading to enhanced conversion rates of recalcitrant biomass.

COMPUTATIONAL METHODS

Simulations were run using CHARMM[30] with the C35 force field[31,32] and TIP3P water.[33,34] The starting structure was originally 24 glucose units long and was equilibrated as previously described by Beckham et al.[5]

For the decrystallization simulations, the structure was trimmed to 14 glucose units for computational efficiency. The longest oligomer examined by this study was eight glucose units long. In addition to hydrolyzing the appropriate bond for the desired oligomer length, the last glucose unit in the oligomer was positioned slightly above the remaining crystallized cellulose strand. Further details regarding system preparation and the MD protocol can be found in the Supporting Information.

The equilibrated systems were used to perform free energy simulations using MD umbrella sampling.[35,36] The reaction coordinate used in these simulations is the fraction of native contacts of the oligomer to the intact crystal.[5,37,43] Here, we define native contacts as the residues within 14 Å of the center of mass of the individual glucose units of the oligomer of interest. The distance cutoff for the native contacts is larger than the nonbonded cutoff distance of 10 Å to ensure that, in the product state, the oligomer does not interact with the cellulose crystal and that the hydration of both the cellulose crystal and oligomer are not affected by the presence of the other. The use of native contacts for polymer decrystallization has been previously discussed.[5,43] Windows were run for 10 ns each from a reaction coordinate of $\rho = 0-1$. A reaction coordinate of 0 (normalized in this case) corresponds to the oligomer in the crystal. A reaction coordinate of 1 corresponds to all of the native contacts being broken with the oligomer free in solution to sample available conformational space. The Supporting Information contains an extended discussion of the reaction coordinate choice and normalization. A total of 21 windows were used for each scenario, yielding a total of 0.21 μs per decrystallization scenario. The umbrella sampling simulations were evaluated for appropriate window overlap and simulation convergence, as shown in Figure S1 (Supporting Information). The PMFs were calculated using the weighted histogram analysis method,[38] and error analysis was performed with bootstrapping. A brief discussion of this technique is included in the Supporting Information.

ASSOCIATED CONTENT

Supporting Information. Decrystallization movie, additional simulation methods, reaction coordinate calculation, root-mean-square fluctuation data, self and interlayer hydrogen bonding, intralayer interaction electrostatics, and van der Waals energies. This material is available free of charge via the Internet at http://pubs.acs.org.

AUTHOR INFORMATION

Corresponding Author

*E-mail: christy.payne@nrel.gov (C.M.P.); gregg.beckham@nrel.gov (G.T.B.).

ACKNOWLEDGMENT

We thank the DOE Office of the Biomass Program for funding. Computer time was provided by the NREL Computational Sciences Center Red Mesa cluster, supported by the DOE Office of EERE under Contract Number DE-AC36-08GO2-8308TACC, and by the Ranger cluster under the National Science Foundation Teragrid Grant Number MCB090159. We acknowledge use of Alan Grossfield's WHAM code.[39] We thank Malin Bergenstråhle, Peter Ciesielski, Bryon Donohoe, Andrew Griggs, James Matthews, and Jakob Wohlert for helpful discussions and a critical reading of the manuscript. All simulation snapshots and movies were made with VMD 1.8.7.[40]

REFERENCES

(1) O'Sullivan, A. C. Cellulose: The Structure Slowly Unravels. *Cellulose* **1997**, *4*, 173–207.

(2) Himmel, M. E.; Ding, S. Y.; Johnson, D. K.; Adney, W. S.; Nimlos, M. R.; Brady, J. W.; Foust, T. D. Biomass Recalcitrance: Engineering Plants and Enzymes for Biofuels Production. *Science* **2007**, *315*, 804–807.

(3) Nishiyama, Y.; Langan, P.; Chanzy, H. Crystal Structure and Hydrogen-Bonding System in Cellulose Iβ. *J. Am. Chem. Soc.* **2002**, *124*, 9074–9082.

(4) Nishiyama, Y.; Sugiyama, J.; Chanzy, H.; Langan, P. Crystal Structure and Hydrogen Bonding System in Cellulose Iα. *J. Am. Chem. Soc.* **2003**, *125*, 14300–14306.

(5) Beckham, G. T.; Matthews, J. F.; Peters, B.; Bomble, Y. J.; Himmel, M. E.; Crowley, M. F. Molecular-Level Origins of Biomass Recalcitrance: Decrystallization Free Energies for Four Common Cellulose Polymorphs. *J. Phys. Chem. B* **2011**, *115*, 4118–4127.

(6) Bergenstråhle, M.; Thormann, E.; Nordgren, N.; Berglund, L. A. Force Pulling of Single Cellulose Chains at the Crystalline Cellulose–Liquid Interface: A Molecular Dynamics Study. *Langmuir* **2009**, *25*, 4635–4642.

(7) Bergenstråhle, M.; Wohlert, J.; Himmel, M. E.; Brady, J. W. Simulation Studies of the Insolubility of Cellulose. *Carb. Res.* **2010**, *345*, 2060–2066.

(8) Peri, S.; Nazmul Karim, M.; Khare, R. Potential of Mean Force for Separation of the Repeating Units in Cellulose and Hemicellulose. *Carbohydr. Res.* **2011**, *346*, 867–871.

(9) Shen, T. Y.; Langan, P.; French, A. D.; Johnson, G. P.; Gnanakaran, S. Conformational Flexibility of Soluble Cellulose Oligomers: Chain Length and Temperature Dependence. *J. Am. Chem. Soc.* **2009**, *131*, 14786–14794.

(10) Gross, A. S.; Chu, J. W. On the Molecular Origins of Biomass Recalcitrance: The Interaction Network and Solvation Structures of Cellulose Microfibrils. *J. Phys. Chem. B* **2010**, *114*, 13333–13341.

(11) Matthews, J. F.; Skopec, C. E.; Mason, P. E.; Zuccato, P.; Torget, R. W.; Sugiyama, J.; Himmel, M. E.; Brady, J. W. Computer Simulations of Microcrystalline Cellulose Iβ. *Carbohydr. Res.* **2006**, *341*, 138–152.

(12) French, A. D.; Johnson, G. P. Advanced Conformational Energy Surfaces for Cellobiose. *Cellulose* **2004**, *11*, 449–462.

(13) French, A. D.; Johnson, G. P. Quantum Mechanics Studies of Cellobiose Conformations. *Can. J. Chem.* **2006**, *84*, 603–612.

(14) French, A. D.; Johnson, G. P. Cellulose and the Twofold Screw Axis: Modeling and Experimental Arguments. *Cellulose* **2009**, *16*, 959–973.

(15) Stortz, C. A.; French, A. D. Disaccharide Conformational Maps: Adiabaticity in Analogues with Variable Ring Shapes. *Mol. Simul.* **2008**, *34*, 373–389.

(16) Yui, T.; Nishimura, S.; Akiba, S.; Hayashi, S. Swelling Behavior of the Cellulose Iβ Crystal Models by Molecular Dynamics. *Carbohydr. Res.* **2006**, *341*, 2521–2530.

(17) Wohlert, J.; Berglund, L. A. A Coarse-Grained Model for Molecular Dynamics Simulations of Native Cellulose. *J. Chem. Theory Comput.* **2011**, *7*, 753–760.

(18) Paavilainen, S.; Rog, T.; Vattulainen, I. Analysis of Twisting of Cellulose Nanofibrils in Atomistic Molecular Dynamics Simulations. *J. Phys. Chem. B* **2011**, *115*, 3747–3755.

(19) Bu, L.; Beckham, G. T.; Crowley, M. F.; Chang, C. H.; Matthews, J. F.; Bomble, Y. J.; Adney, W. S.; Himmel, M. E.; Nimlos, M. R. The Energy Landscape for the Interaction of the Family 1 Carbohydrate-Binding Module and the Cellulose Surface Is Altered by Hydrolyzed Glycosidic Linkages. *J. Phys. Chem. B* **2009**, *113*, 10994–11002.

(20) Zhang, Y. H. P.; Lynd, L. R. A Functionally Based Model for Hydrolysis of Cellulose by Fungal Cellulase. *Biotechnol. Bioeng.* **2006**, *94*, 888–898.

(21) Zhou, W.; Schuttler, H. B.; Hao, Z. Q.; Xu, Y. Cellulose Hydrolysis in Evolving Substrate Morphologies I: A General Modeling Formalism. *Biotechnol. Bioeng.* **2009**, *104*, 261–274.

(22) Zhou, W.; Hao, Z. Q.; Xu, Y.; Schuttler, H. B. Cellulose Hydrolysis in Evolving Substrate Morphologies II: Numerical Results and Analysis. *Biotechnol. Bioeng.* **2009**, *104*, 275–289.

(23) Levine, S. E.; Fox, J. M.; Blanch, H. W.; Clark, D. S. A Mechanistic Model of the Enzymatic Hydrolysis of Cellulose. *Biotechnol. Bioeng.* **2010**, *107*, 37–51.

(24) Bansal, P.; Hall, M.; Realff, M. J.; Lee, J. H.; Bommarius, A. S. Modeling Cellulase Kinetics on Lignocellulosic Substrates. *Biotech. Adv.* **2009**, *27*, 833–848.

(25) Jalak, J.; Valjamae, P. Mechanism of Initial Rapid Rate Retardation in Cellobiohydrolase Catalyzed Cellulose Hydrolysis. *Biotechnol. Bioeng.* **2010**, *106*, 871–883.

(26) Huebner, A.; Ladisch, M. R.; Tsao, G. T. Preparation of Cellodextrins — Engineering Approach. *Biotechnol. Bioeng.* **1978**, *20*, 1669–1677.

(27) Gray, M. C.; Converse, A. O.; Wyman, C. E. Sugar Monomer and Oligomer Solubility — Data and Predictions for Application to Biomass Hydrolysis. *Appl. Biochem. Biotechnol.* **2003**, *105*, 179–193.

(28) Chundawat, S. P. S.; Beckham, G. T.; Himmel, M. E.; Dale, B. E. Deconstruction of Lignocellulosic Biomass to Fuels and Chemicals. *Ann. Rev. Chem. Biomolec. Eng.* **2011**, *2*, DOI: 10.1146/annurev-chembioeng-061010-114205.

(29) Beckham, G. T.; Bomble, Y. J.; Bayer, E. A.; Himmel, M. E.; Crowley, M. F. Applications of computational science for understanding enzymatic deconstruction of cellulose. *Curr. Opin. Biotechnol.* **2011**, *22*, 231–238.

(30) Brooks, B. R.; Brooks, C. L., 3rd; Mackerell, A. D., Jr.; Nilsson, L.; Petrella, R. J.; Roux, B.; Won, Y.; Archontis, G.; Bartels, C.; Boresch, S.; et al. CHARMM: The Biomolecular Simulation Program. *J. Comput. Chem.* **2009**, *30*, 1545–1614.

(31) Guvench, O.; Greene, S. N.; Kamath, G.; Brady, J. W.; Venable, R. M.; Pastor, R. W.; Mackerell, A. D. Additive Empirical Force Field for Hexopyranose Monosaccharides. *J. Comput. Chem.* **2008**, *29*, 2543–2564.

(32) Guvench, O.; Hatcher, E.; Venable, R. M.; Pastor, R. W.; MacKerell, A. D. CHARMM Additive All-Atom Force Field for Glycosidic Linkages Between Hexopyranoses. *J. Chem. Theory Comput.* **2009**, *5*, 2353–2370.

(33) Jorgensen, W. L.; Chandrasekhar, J.; Madura, J. D.; Impey, R. W.; Klein, M. L. Comparison of Simple Potential Functions for Simulating Liquid Water. *J. Chem. Phys.* **1983**, *79*, 926–935.

(34) Durell, S. R.; Brooks, B. R.; Ben-Naim, A. Solvent-Induced Forces between 2 Hydrophilic Groups. *J. Phys. Chem.* **1994**, *98*, 2198–2202.

(35) Torrie, G. M.; Valleau, J. P. Non-Physical Sampling Distributions in Monte-Carlo Free-Energy Estimation — Umbrella Sampling. *J. Comput. Phys.* **1977**, *23*, 187–199.

(36) Kottalam, J.; Case, D. A. Dynamics of Ligand Escape from the Heme Pocket of Myoglobin. *J. Am. Chem. Soc.* **1988**, *110*, 7690–7697.

(37) Sheinerman, F. B.; Brooks, C. L. Calculations on Folding of Segment B1 of Streptococcal Protein G. *J. Mol. Biol.* **1998**, *278*, 439–456.

(38) Kumar, S.; Rosenberg, J. M.; Bouzida, D.; Swendsen, R. H.; Kollman, P. A. The Weighted Histogram Analysis Method for Free-Energy Calculations on Biomolecules. I. The Method. *J. Comput. Chem.* **1992**, *13*, 1011–1021.

(39) Grossfield, A. *An Implementation of WHAM: The Weighted Histogram Analysis Method*, 2.0.5 ed.; 2003.

(40) Humphrey, W.; Dalke, A.; Schulten, K. VMD — Visual Molecular Dynamics. *J. Mol. Graphics* **1996**, *14*, 33–38.

(41) Roberts, K. M; Lavenson, D. M; Tozzi, E. J.; McCarthy, M. J. The Effect of Water Interactions in Cellulose Suspensions on Mass Transfer and Saccharification Efficiency at High Solids Loadings. *Cellulose* **2011**, *19*, 759–773.

(42) Kristensen, J. B; Felby, C.; Jørgensen, H. Yield-Determining Factors in High-Solids Enzymatic Hydrolysis of Lignocellulose. *Biotech. Biofuel.* **2009**, *2*, 11.

(43) Beckham, G. T; Crowley, M. F. Examination of the a-Chitin Structure and Decrystallization Thermodynamics at the Nanoscale. *J. Phys. Chem. B* **2011**, *115*, 4516–4522.